Buoyancy-driven convection around exothermic autocatalytic chemical fronts traveling horizontally in covered thin solution layers

L. Rongy[a] and A. De Wit
Nonlinear Physical Chemistry Unit and Center for Nonlinear Phenomena and Complex Systems, CP 231, Faculté des Sciences, Université Libre de Bruxelles (ULB), Brussels 1050, Belgium

(Received 5 December 2008; accepted 13 October 2009; published online 9 November 2009)

Spatial variations of concentrations and temperature across exothermic chemical fronts can initiate buoyancy-driven convection. We investigate here theoretically the spatiotemporal dynamics arising from such a coupling between exothermic autocatalytic reactions, diffusion, and buoyancy-driven flows when an exothermic autocatalytic front travels perpendicularly to the gravity field in a thin solution layer. To do so, we numerically integrate the incompressible Stokes equations coupled to evolution equations for the concentration of the autocatalytic product and temperature through buoyancy terms proportional to, respectively, a solutal R_C and a thermal R_T Rayleigh number. We show that exothermic fronts can exhibit new types of dynamics in the presence of convection with regard to the isothermal system. In the cooperative case (R_C and R_T are of the same sign), the dynamics asymptotes to one vortex surrounding, deforming, and accelerating the front much like in the isothermal case. However, persistent local stratification of heavy zones over light ones can be observed at the rear of the front when the Lewis number *Le* (ratio of thermal diffusivity over molecular diffusion) is nonzero. When the solutal and thermal effects are antagonistic (R_C and R_T of opposite sign), temporal oscillations of the concentration, temperature, and velocity fields can, in some cases, be observed in a reference frame moving with the front. The various dynamical regimes are discussed as a function of R_C, R_T, and *Le*. © *2009 American Institute of Physics*.
[doi:10.1063/1.3258277]

I. INTRODUCTION

Density changes across an autocatalytic reaction-diffusion (RD) front traveling in the gravity field can trigger buoyancy-driven convection.[1] Indeed, chemical reactions can change the density ρ of the solution either by modifying the total volume of products versus reactants or by releasing or consuming heat.[1–3] These two effects provide, respectively, a solutal ($\Delta\rho_S$) and a thermal ($\Delta\rho_T$) contribution to the total density change defined as $\Delta\rho=\rho(\text{products})-\rho(\text{reactants})$. Since no endothermic autocatalytic reactions are known up to now the thermal contribution $\Delta\rho_T<0$ is here always negative as reactions are exothermic. All autocatalytic fronts can then be classified in two categories depending on whether the solutal and thermal effects are *cooperative* (both $\Delta\rho_S$ and $\Delta\rho_T<0$) or *antagonistic* ($\Delta\rho_S>0$ and $\Delta\rho_T<0$).[2,4]

The dynamics of buoyantly unstable exothermic fronts have been thoroughly studied in the case where the front travels parallel to the gravity field. In that configuration, the system is either directly unstable (Rayleigh–Taylor instability[1,2,4]) or the competition between antagonistic solutal and thermal buoyancy effects can lead to multicomponent convection (double-diffusive instabilities).[4,5] In this case, even though the overall density gradient is statically stable, convection can set in because of the difference between heat and mass diffusivities.[2,4–7] For example, competing solutal and thermal effects in the chlorite-tetrathionate (CT) reaction can lead to the destabilization of otherwise stable fronts and to new types of fingering in vertical geometries.[4,6–10,36] In the cooperative situation, solutal and thermal effects are reinforcing each other but can nevertheless lead to new dynamics in vertical geometries where buoyancy-driven instabilities of initially statically stable fronts can occur.[4,7,11]

On the contrary, if the front travels horizontally (perpendicular to the gravity field), any density difference across the front always leads to buoyancy-induced flows, with the heavier solution naturally sinking below the lighter one. Experiments have indeed shown that autocatalytic fronts propagating in horizontal tubes can travel faster than in gels[1,12–15] and be deformed by convection.[14–16,35] In the exothermic chlorite-thiourea-barium chloride reaction system, convection has also been shown experimentally to influence the autocatalytic wave traveling horizontally in a Petri dish open to air.[17–20] Formation of patterns and of thermal plumes is there certainly influenced by thermal effects. The dynamics has been qualitatively discussed in terms of coupling between surface tension-driven (Marangoni) flows and buoyancy-driven multicomponent convection, via the formation of convective tori at the wave front. To gain insight into these intricate front dynamics occurring in horizontal solution layers, several theoretical works analyzed the influence on isothermal chemical fronts of pure solutal buoyancy-driven convection on the one hand[21–23] and of pure solutal Marangoni-driven convection on the other hand.[24–28]

In this context, the purpose of this article is to address the additional influence of thermal effects on buoyancy-

[a]Electronic mail: lrongy@ulb.ac.be and adewit@ulb.ac.be.

driven convection around exothermic fronts traveling in a horizontal closed system, i.e., in the absence of interfacial Marangoni stresses. To do so, we numerically analyze the dynamics of such fronts when density differences due to both compositional and thermal changes act across the front to trigger buoyancy convection. The fact that heat diffuses more rapidly than mass and the possible competition between antagonistic solutal and thermal buoyancy effects lead to interesting new dynamics in comparison to the isothermal system.[35]

To investigate this situation, the incompressible Stokes equations for the velocity field are coupled through buoyancy terms to the RD-convection (RDC) equations for the temperature T and the concentration c of the autocatalytic product of the reaction. The density of the solution is supposed to vary linearly with c and T, which, respectively, introduces a solutal R_C and a thermal R_T Rayleigh number. We first consider the dynamics of cooperative systems where solutal and thermal effects both contribute to a decrease in the density during the reaction (solute lighter and hotter products: R_C, $R_T>0$). We next consider a system where the two effects are antagonistic ($R_C<0$ and $R_T>0$) involving solute heavier but hotter products. We show that new dynamics can develop both when thermal and solutal effects act cooperatively or antagonistically. A new oscillatory behavior occurs for some parameter ranges in the antagonistic regime. Influence of the solutal and thermal Rayleigh numbers as well as of the Lewis number, measuring the ratio between thermal and molecular diffusivity, are investigated.

The article is organized according to the following outline. In Sec. II, we present our two-dimensional (2D) model system and briefly recall the properties of the pure RD fronts. In Sec. III, the nonlinear dynamics of the exothermic system is presented and compared with the isothermal results obtained in a previous study.[23] Conclusions are drawn in Sec. IV.

II. MODEL SYSTEM

A. Equations of motion

We consider a 2D thin aqueous solution layer of length L_x and height L_z, corresponding to a vertical cut in a covered rectangular channel oriented horizontally in the gravity field $\underline{g}$ with z pointing upwards and x horizontally. The system is closed at each side and has thus no free surface which excludes any Marangoni effects. An exothermic autocatalytic reaction takes place in the solution following the global irreversible kinetics, $A+2C\rightarrow 3C$. When coupled to diffusion, this kinetics yields a planar RD front of concentration and temperature separating the reacted and unreacted solutions and propagating along the x direction. The density of the products differs from that of the reactants since these two states correspond to different concentrations and temperature. The resulting horizontal density gradients across the front induce convective motions in the solution which in turn affect the RD dynamics. Therefore, the governing equations describing the temporal evolution of this system are obtained by coupling the incompressible Stokes equations in the Boussinesq approximation (1) and (2) for the evolution of the 2D velocity field $\underline{v}=(u,w)$ to RDC equations for the concentration c of the product (3) and for the temperature T [Eq. (4)]. The chemical production term is taken as $f(c)=kc^2(a_0-c)$, where k is the rate constant and a_0 is the initial reactant concentration. This kinetics is able to describe autocatalytic chemical systems such as the iodate-arsenous acid (IAA) redox reaction[22,23,29–32] for instance. The density of the diluted solution $\rho(c,T)$ is assumed to be a linear function of both c and T [see Eq. (5)]. Namely, our model reads

$$\underline{\nabla} p = \mu \nabla^2 \underline{v} + \rho(c,T)\underline{g}, \tag{1}$$

$$\underline{\nabla} \cdot \underline{v} = 0, \tag{2}$$

$$\frac{\partial c}{\partial t} + \underline{v} \cdot \underline{\nabla} c = D\nabla^2 c + f(c), \tag{3}$$

$$\rho_0 c_p \left(\frac{\partial T}{\partial t} + \underline{v} \cdot \underline{\nabla} T \right) = \kappa_T \nabla^2 T - \Delta H f(c), \tag{4}$$

$$\rho(c,T) = \rho_0 + \frac{\partial \rho}{\partial c} c + \frac{\partial \rho}{\partial T}(T - T_0), \tag{5}$$

where p denotes the pressure, and $\underline{g}=(0,-g)$ is the gravity acceleration acting along z. The solutal and thermal expansion coefficients $\partial\rho/\partial c$ and $\partial\rho/\partial T$ are assumed constant, and $\rho_0=\rho(c=0,T=T_0)$ is the density of the initial reactant solution, with T_0 as the ambient temperature before reaction. The specific heat capacity of the solution c_p, its thermal conductivity κ_T, its dynamic viscosity μ, the reaction enthalpy ΔH (negative here because the reaction is exothermic), the molecular diffusion coefficient D, and the kinetic constant k are assumed to be constant.

The dimensionless equations are obtained by using the characteristic scales of the RD system: for time, $\tau_c=1/ka_0^2$, for length, $L_c=\sqrt{D\tau_c}$, for velocity, $U_c=L_c/\tau_c=\sqrt{D/\tau_c}$, and for concentration, a_0. The enthalpy of the reaction leads to an adiabatic temperature rise ΔT in the reaction zone from the ambient temperature T_0 before reaction to $T_0+\Delta T$ where $\Delta T=-\Delta H a_0/(\rho_0 c_p)$ is positive since the considered autocatalytic reaction is exothermic. We define a dimensionless temperature as $T'=(T-T_0)/\Delta T$. The pressure is scaled by $p_c=\mu/\tau_c$, so that the dimensionless pressure $p'=p/p_c$. In addition, we define a new pressure gradient incorporating the hydrostatic pressure gradient term as $\underline{\nabla}' p''=\underline{\nabla}' p' - \rho_0 L_c \underline{g}/p_c$, which is used in Eq. (6) where the primes have been dropped. The dimensionless density is defined as $\rho'=(\rho-\rho_0)/\rho_c$, where $\rho_c=p_c/L_c g$. The dimensionless governing equations read

$$\underline{\nabla} p = \nabla^2 \underline{v} + (R_C c + R_T T)\underline{i_z}, \tag{6}$$

$$\underline{\nabla} \cdot \underline{v} = 0, \tag{7}$$

$$\frac{\partial c}{\partial t} + \underline{v} \cdot \underline{\nabla} c = \nabla^2 c + c^2(1-c), \tag{8}$$

$$\frac{\partial T}{\partial t} + \underline{v} \cdot \underline{\nabla} T = Le \nabla^2 T + c^2(1-c), \tag{9}$$

where $\underline{i}_z$ is the unit vector in the z-direction and the Lewis number, $Le = D_T/D$, is the ratio between the thermal diffusivity $D_T = \kappa_T/(\rho_0 c_p)$ and the molecular diffusivity D. The dimensionless solutal and thermal Rayleigh numbers, R_C and R_T, are defined, respectively, as

$$R_C = -\frac{\partial \rho}{\partial c}\frac{a_0 L_c^3 g}{D\mu}, \tag{10}$$

$$R_T = -\frac{\partial \rho}{\partial T}\frac{\Delta T L_c^3 g}{D\mu}. \tag{11}$$

The solutal Rayleigh number R_C is positive if the product decreases the density in the course of reaction and negative otherwise while the thermal Rayleigh number R_T is always positive since the reaction is exothermic ($\Delta T > 0$) and we work at room temperature ($\partial\rho/\partial T$ is negative for water at $T > 4$ °C). To avoid any confusion, we will speak here about solute heavier or lighter when referring to a solutal contribution to the density difference. The dimensionless density field is then explicitly obtained as

$$\rho(x,z,t) = -R_C c(x,z,t) - R_T T(x,z,t). \tag{12}$$

Ahead of the front, the reactants (where $c = T = 0$) have a dimensionless density $\rho_r = 0$ due to our choice of nondimensionalization, while the dimensionless density of the products behind the front (where $c = T = 1$) is $\rho_p = -R_C - R_T$.

Numerical simulations of Eqs. (6)–(9) are carried out in a domain of dimensionless height L_z and width L_x using the numerical procedure described in Ref. 23. At each boundary of the domain we require zero-flux boundary conditions for the chemical concentration c and the temperature T. Indeed, we assume that the system is thermally insulated and the reactor operates adiabatically, therefore neglecting effects of possible heat losses through the system boundaries.[33,34] The hydrodynamic boundary conditions are rigid walls with no slip for the vertical boundaries and slip walls for the horizontal boundaries, i.e.,

$$\frac{\partial c}{\partial x} = \frac{\partial T}{\partial x} = u = \frac{\partial w}{\partial x} = 0 \quad \text{at} \quad x = 0, \quad x = L_x, \tag{13}$$

$$\frac{\partial c}{\partial z} = \frac{\partial T}{\partial z} = u = w = 0 \quad \text{at} \quad z = 0, \quad z = L_z, \tag{14}$$

The length of the system and slip walls do not influence the results as long as the reactor length is taken sufficiently long for the front not to interact with a lateral boundary on the time of interest.

B. Traveling concentration and temperature fronts

In the absence of flow, i.e., for Rayleigh numbers equal to zero, the RD equation for the concentration (8), with $\underline{v} = \underline{0}$ and boundary conditions $c \to 1$ as $x \to -\infty$ and $c \to 0$ as $x \to +\infty$, admits as solution the following propagating front:[29–31]

$$c(x,t) = \frac{1}{1+e^{(x-vt)/\sqrt{2}}} = \frac{1}{2}\left[1 + \tanh\left(-\frac{\sqrt{2}}{4}(x-vt)\right)\right], \tag{15}$$

where $v = \sqrt{2}/2$ is the constant RD speed of the front. This profile connects the kinetically stable product $c = 1$ to the invaded $c = 0$ solution corresponding to the reactants. The width w_{RD} of this front, arbitrarily defined as the distance between $c = 0.99$ and $c = 0.01$, equals $w_{RD} = 2\sqrt{2}\ln 99 \sim 13$.

As the reaction is exothermic, the concentration front generates a heat front traveling at the same RD speed v independent of the Lewis number. If $Le = 1$, the solution for the temperature Eq. (9) is the same as for the concentration equation, i.e., the heat front profile is described by the analytical solution (15) in the absence of convection. However, for aqueous solutions, the Lewis number is larger than one since, in water, heat diffuses faster than mass. To evaluate the Lewis number $Le = D_T/D$, we use the value of the thermal diffusivity in water, $D_T = 1.42 \times 10^{-3}$ cm^2/s, and two typical values of the molecular diffusivity: i.e., $D = 2.0 \times 10^{-5}$ cm^2/s in the IAA reaction,[13] and $D = 1.2 \times 10^{-4}$ cm^2/s in the CT reaction.[8] This gives a Lewis number $Le \sim 70$ for the IAA system and $Le \sim 10$ for the CT system. For such $Le > 1$, an explicit analytical front solution cannot be obtained so that a numerical integration of Eqs. (8) and (9) with $\underline{v} = \underline{0}$ and zero-flux boundary conditions is used to obtain the RD temperature profile. Heat diffusing faster than mass, the width of the temperature front is much larger than the one of the concentration front as seen in Fig. 1(a). Typical temperature differences across autocatalytic fronts in aqueous solutions[3,8,13] are between 0.4 and 3 K with a thermal density jump of the same order as the solutal one, $\sim 10^{-4}$ g/cm^3. Figure 1(b) shows examples of density profiles reconstructed from Eq. (12) in the cooperative case with solutal and thermal Rayleigh numbers of the same magnitude and sign, i.e., when solutal and thermal effects act cooperatively to decrease the density during the reaction. The products located behind the front are solute lighter and hotter than the reactants so that the density profiles are monotonous increasing functions along x. Logically, these profiles are also more spread out when the Lewis number increases.

III. BUOYANCY-DRIVEN FLOWS AROUND EXOTHERMIC FRONTS

To get insight into the influence of buoyancy-driven convection on the RDC dynamics of exothermic fronts propagating in horizontal solution layers, we numerically integrate Eqs. (6)–(9) with boundary conditions (13) and (14) and with steplike functions for c and T as initial condition. The three important parameters of the problem are the two Rayleigh numbers, R_C and R_T, and the Lewis number Le. The role of the layer thickness on the isothermal buoyancy-driven flow has been addressed in a previous study.[23] There, it has been shown that the intensity of convection increases with L_z which is observed to be the case for the thermal situation too.[35] Hence, throughout this paper, we consider a quite thin layer of one millimeter in thickness, which is more or less

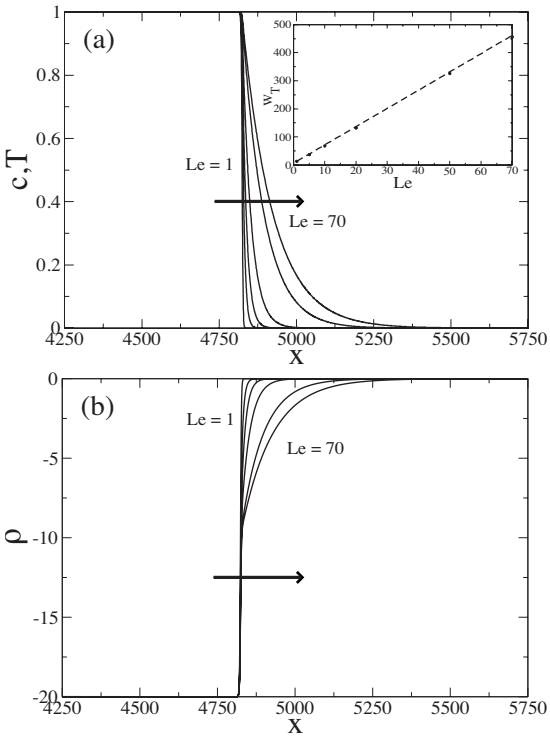

FIG. 1. (a) Temperature profiles along the direction of propagation x for different Lewis numbers $Le=1$, 5, 10, 20, 50, 70, from left to right. The concentration profile does not depend on Le and is superimposed to the temperature profile obtained for $Le=1$. Inset: RD width w_T of the temperature front (defined as the distance between $T=0.01$ and $T=0.99$) as a function of Le. The broken line corresponds to a linear fit to the numerical data, $w_T=0.5(Le+1)w_T^{(Le=1)}$. (b) Density profiles along x reconstructed for the cooperative case $R_C=R_T=10$ and the same values of Le as in (a). During the reaction, the density evolves from $\rho_r=0$ for the reactants to $\rho_p=-R_C-R_T$ for the products. The arrows indicate the direction of the front propagation.

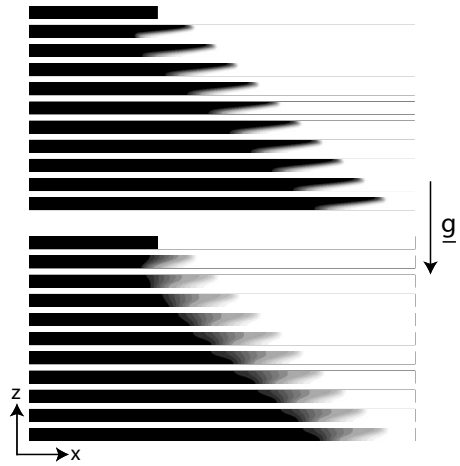

FIG. 2. Evolution of the concentration (top) and the temperature (bottom) fronts propagating in the presence of solutal and thermal buoyancy convection for $R_C=R_T=10$ and $Le=5$, shown from top to bottom from $t=0$ up to $t=50$ with a time interval of $\Delta t=5$. The concentration and temperature fields are shown on a gray scale between black corresponding to the hotter products and white for the colder reactants. The length of the integration domain is equal to $L_x=512$ and the initial condition is localized at $x=100$. In this figure, the aspect ratio between $L_x=300$ (we only show $300L_c$ out of $512L_c$ to focus on the reaction zone) and $L_z=10$ is preserved.

the width of an autocatalytic chemical front.[29] In dimensionless variables, this corresponds to a fixed $L_z=10$.

We note that if the Lewis number equals 1, the concentration and temperature fields follow the same solutions and the solutal and thermal effects are strictly additive. The dynamics of an exothermic front characterized by a pair of Rayleigh numbers (R_C,R_T) is in that case identical to the dynamics of an isothermal front as studied in Ref. 23, characterized by a total effective Rayleigh number equal to the sum R_C+R_T. This is true for both cooperative and antagonistic situations. We now examine cases for $Le\neq 1$.

A. Cooperative effects

The cooperative situation, $\Delta\rho_S$ and $\Delta\rho_T<0$, corresponds typically to the case of the IAA reaction.[2,4] Both solutal and thermal Rayleigh numbers are positive and the products are thus lighter than the reactants since they are both solute lighter and hotter.

As said above, if $Le=1$ then the dynamics is the same as that of isothermal fronts with an effective Rayleigh number equal to R_C+R_T. The density difference across the front triggers then for $R_C+R_T>0$ an asymptotic dynamics in which a clockwise rotating vortex deforms the front and travels with it at a constant faster RDC speed. This vortex is entrained by the motion of the lighter products rising above the heavier reactants. The situation is however slightly different when $Le\neq 1$. As in the isothermal situation,[23] the system still reaches an asymptotic RDC dynamics characterized by a steady fluid flow traveling at a constant speed with the exothermic front featuring a steady deformed shape across the layer. As an example, the temporal evolution toward the asymptotic regime of c and T is shown in Fig. 2 for equal solutal and thermal Rayleigh numbers, $R_C=R_T=10$, and $Le=5$. The temperature and concentration fronts are first deformed alike with the heavy and cold reactants sinking below the light and hot products rising to the top. However, the temperature front next develops an additional deformation at the rear where an unexpected stratification of hot products below a colder intermediate zone between reactants and products is observed. The front reaches a steady propagating state after around $40\tau_c-50\tau_c$ and the asymptotic fluid flow corresponds to a convection roll localized in the front region as shown in Fig. 3 with however the presence of a hot spot at the rear of the front in the bottom part of the layer. This hot spot is due to a locally higher reaction rate at the location where the clockwise rotating vortex brings in fresh reactants in contact with the autocatalytic product.[36]

Since solutal and thermal effects are cooperative, the presence of a hot spot at the bottom of the product region where the concentration is homogeneous corresponds to a stratification of a lighter solution under a heavier one localized at the rear of the front and propagating at a constant speed. This locally buoyantly unfavorable stratification is somehow stabilized and remains steady in the comoving frame as can be seen in Fig. 3(c) where the density of the solution has been reconstructed from the asymptotic concentration and temperature fields following Eq. (12).

1. Influence of the Rayleigh numbers

Increasing the Rayleigh numbers at a fixed Lewis number results for cooperative systems in a larger deformation of

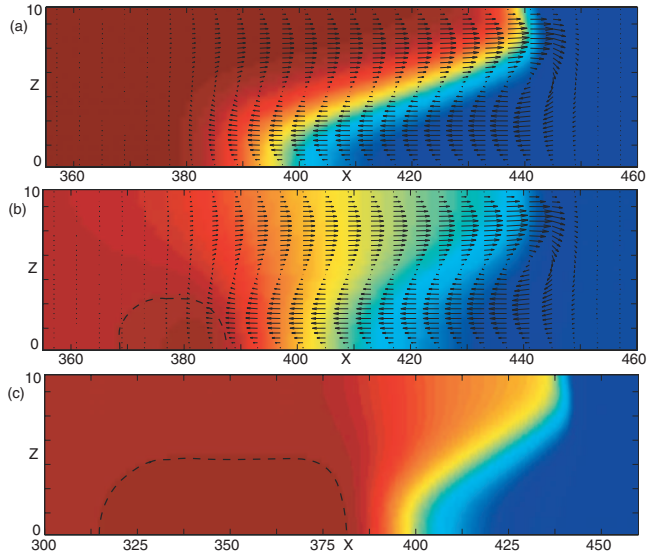

FIG. 3. Focus on the convection roll of Fig. 2 traveling with the deformed front and superimposed on the concentration field (a) and temperature field (b), for the cooperative case $R_C=R_T=10$ and $Le=5$. These figures are shown at $t=100$ and represent the solute lighter and hotter products, $c=T=1$, in red invading the solute heavier and colder reactants, $c=T=0$, in blue. The maximum temperature, $T=1.04$, is the temperature of the hot spot at the rear of the front and is shown in dark red. The z-direction has been magnified in order to see the details of the velocity field. (c) Focus on the density field in the reaction zone shown at $t=100$ for the same parameters as in (a) and (b). The density ranges from its minimum value, $\rho_{\min}=-20.2$, in red to its maximum value, $\rho_{\max}=0.0$, in blue. The dashed lines have been added to highlight the hot spot at the rear of the front.

the front across the layer, a stronger fluid flow, and a larger propagation speed of the RDC structure, similarly to the isothermal case.[23] For a fixed sum R_C+R_T and $Le>1$, the buoyancy-induced convection and the corresponding effects of convection on the front properties become smaller when the relative influence of the thermal versus solutal effects increase (increasing R_T/R_C). Indeed, as the temperature front is wider than the concentration one, the resulting gradient in density for a same value of the total Rayleigh number is then smaller. The hot spot traveling with the exothermic front in the asymptotic regime is always localized in the bottom part of the layer (cf. Fig. 3) and its amplitude is proportional to the ratio R_C/R_T rather than to the intensity of convection.

2. Influence of the Lewis number

In the cooperative case, the system dynamics evolves for every Le studied here ($1\leq Le\leq 70$) toward a steady regime, reached after $50\tau_c$ and featuring a deformed front propagating at a constant speed and surrounded by a steady fluid vortex. Figure 4 presents four properties of the system characterizing the asymptotic regime for various Lewis numbers. The deformation of the front by convection is quantified by the mixing length of the concentration front, W_c, and of the temperature front, W_T, respectively, defined as the distance between $\langle c(x,t)\rangle=0.01$ and $\langle c(x,t)\rangle=0.99$ and between $\langle T(x,t)\rangle=0.01$ and $\langle T(x,t)\rangle=0.99$, i.e., between the tip and the rear of the corresponding transversely averaged profile

$$\langle c(x,t)\rangle=\frac{1}{L_z}\int_0^{L_z}c(x,z,t)dz, \tag{16}$$

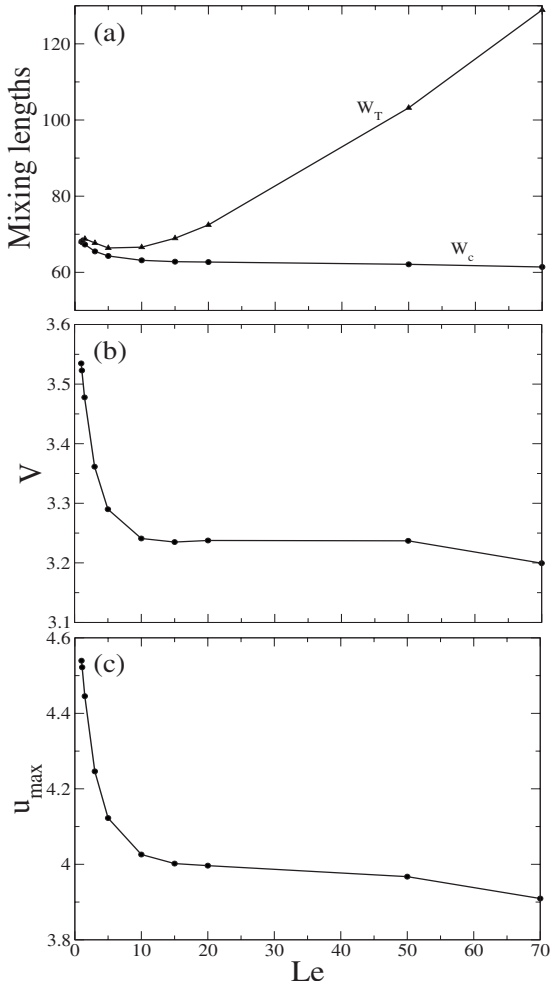

FIG. 4. Asymptotic values of (a) the RDC mixing lengths, W_c and W_T, of the concentration and temperature fronts, respectively, (b) nonlinear RDC propagation speed V, and (c) horizontal velocity with maximum intensity $u_{\max}$ as a function of the Lewis number for the cooperative case $R_C=R_T=10$.

$$\langle T(x,t)\rangle=\frac{1}{L_z}\int_0^{L_z}T(x,z,t)dz. \tag{17}$$

V is the constant RDC propagation speed of both fronts and has been obtained by measuring the slope of the position of the tip of each front as a function of time. $u_{\max}$ is the horizontal velocity u with maximum intensity in the asymptotic RDC regime.

The intensity of convection decreases with Le since wider temperature fronts give rise to smaller density gradients and hence smaller induced fluid velocities. As a result, the deformation of the concentration front quantified by W_c and the propagation speed V are both reduced when Le increases. However, the impact of Le on these asymptotic properties is not strong since multiplying Le by 70 only corresponds to a decrease of 14% in $u_{\max}$ and 10% in W_c and V. Furthermore, the strongest decrease occurs at small Lewis numbers while for $Le\geq 10$, these properties are nearly constant.

On the contrary, the mixing length of the temperature front, W_T, is much more affected by the Lewis number [see Fig. 4(a)]. First we note that there is a value of Le (between

5 and 10) for which the deformation of the temperature front is minimum. The presence of this minimum comes from two opposite tendencies when Le increases: (i) a larger thermal diffusion coefficient D_T gives rise to wider fronts and hence larger W_T; (ii) consequently smaller density gradients and hence smaller convection result in a less pronounced deformation of the front and thus smaller W_T. For $Le \geq 10$, the diffusive effect is stronger than the convective one and the mixing length therefore increases with Le. For large Lewis numbers, the RD width of the thermal front in the absence of flow much exceeds the deformation generated by convection [compare the width w_T of the RD thermal front in Fig. 1(a) with the convection-induced deformation W_C of the concentration front in Fig. 4(a)] so that the mixing length is no longer a measure of the front deformation across the layer but rather measures the width of the front. Furthermore, for large Lewis numbers, diffusion smoothes out the vertical gradients induced by convection with the result that the temperature front is nearly flat. In those cases, convection causes an important sharpening of the front, for example, $W_T=129$ for $Le=70$ with convection against 456 in the absence of convection.

For all the Lewis numbers considered here ($1 \leq Le \leq 70$) except for $Le=1$, a hot spot is present in the RDC dynamics at the rear of the front in the bottom of the layer. Its intensity is maximum between $Le=1.5$ and $Le=5$ and decreases with large Lewis numbers since diffusion tends to smooth it out. Oppositely to the case shown in Fig. 3(c) for $Le=5$, the presence of a hot spot in the bottom of the layer does not give rise to a stable stratification of a heavy solution on top of a lighter one for $Le \geq 20$ since it is compensated by a less concentrated region near the layer bottom.

We end this section by noting that the buoyancy-driven flow field is identical for $Le=1$, $R_C=R_T=10$, and for $Le \neq 1$, $R_C=20$, $R_T=0$ since both of them correspond to the isothermal situation with a Rayleigh number equals 20. However, in the first case, the temperature field is the same as the concentration one while in the second case, there is a region in the bottom of the layer where T exceeds one. A Lewis number larger than one ($D_T > D$) is therefore a prerequisite to the existence of a hot spot even if the contrary would have been expected for a faster diffusing variable.

B. Antagonistic effects

The antagonistic situation, $\Delta\rho_S > 0$ and $\Delta\rho_T < 0$, corresponds typically to the case of the CT reaction[4,8,9] and involves solute heavier but hotter products characterized by a negative solutal Rayleigh number and a positive thermal one.

The most striking feature of the antagonistic case is the time dependence of the asymptotic dynamics when $|R_T|$ is sufficiently larger than $|R_C|$. Competing solutal and thermal effects can then lead to an oscillating dynamics in a frame propagating at a constant speed V as shown in Figs. 5–8, which show the concentration and temperature dynamics and the corresponding oscillating velocity field at different times of one oscillation period. The mechanism of these oscillations can be understood as follows. For the parameter values of Figs. 5–8, the solute heavier products are hot enough to be initially lighter than the reactants and the density to be an increasing function of x. Therefore, the less dense products rise on top of the layer resulting locally in a stratification of a lighter solution on top of a heavier one at the tip of the front. However, as heat diffuses faster than mass, these products on top rapidly cool down which leaves locally solute heavier products above reactants. These products therefore start to sink in the gravity field, forming the descending tongue observed in Figs. 5, 7, and 8. On the contrary, the

FIG. 5. Oscillatory propagation of the concentration front in the presence of competing solutal and thermal buoyancy effects for $R_C=-10$, $R_T=15$, and $Le=5$ shown from top to bottom from $t=0$ up to $t=60$ with a time interval of $\Delta t=3$ ($V=1.50$). The initial condition is at $x=100$ and the aspect ratio between $L_x=256$ and $L_z=10$ is preserved.

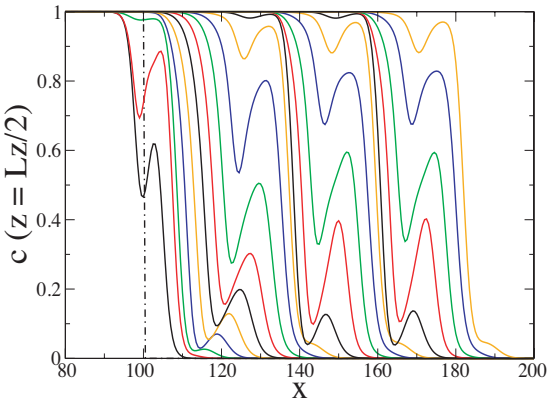

FIG. 6. Concentration profiles along x at $z=L_z/2$ from $t=0$ up to $t=60$ with a time interval of $\Delta t=3$ between two successive curves, for $R_C=-10$, $R_T=15$, and $Le=5$. The dot-dashed curve is the initial condition and the cycle of color is repeated for each oscillation.

FIG. 7. Propagation of the temperature front for the same parameters as in Fig. 5.

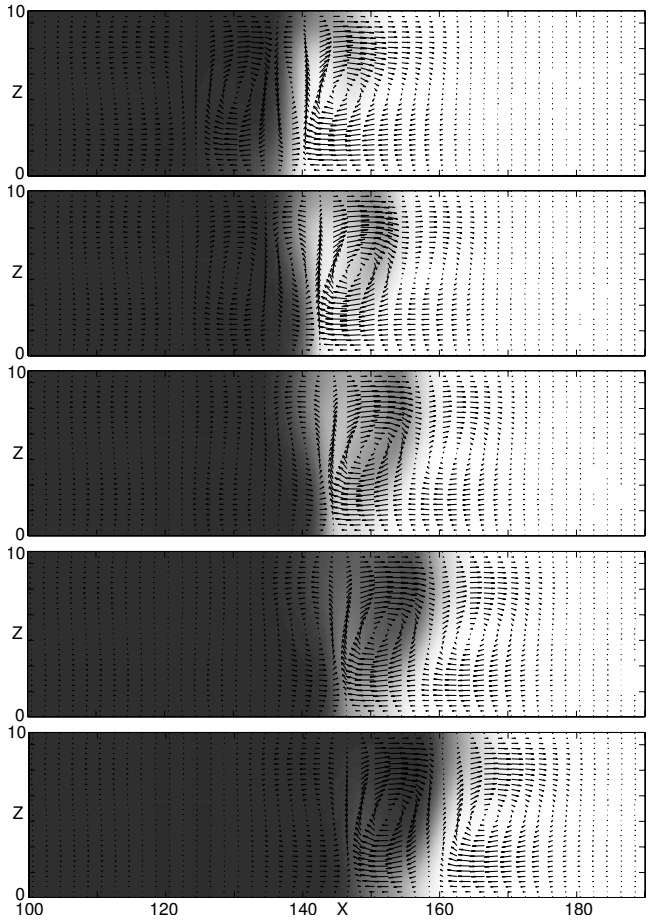

FIG. 8. Focus on the oscillating fluid velocity field traveling at a constant speed with the concentration front for $R_C=-10$, $R_T=15$, and $Le=5$. The structures are shown at $t=33$, 36, 39, 42, 45, top to bottom and correspond to zooms on Fig. 5. The hot but solute heavier products, $c=1$, are shown in black invading the cold but solute lighter reactants, $c=0$, shown in white. The z-direction has been magnified in order to see the details of the velocity field but the velocity vectors are displayed at the same scale in the five plots.

reactants which are already solute lighter than the products are heated up and rise behind the sinking tongue of products as shown in the first three images of Fig. 8. These reactants find themselves surrounded by products in a region where the autocatalytic reaction is therefore enhanced. They are thus swiftly converted into products (see the last two images of Fig. 8) restoring a less deformed interface between reactants and products. The globally lighter products then rise again in the gravity field and the previous cycle repeats itself. The system rapidly reaches a dynamical state propagating at a constant speed V more than twice the RD speed. The front deformation repeats itself with a period of $15\tau_c$ (see Fig. 6) and we note that the velocity field is made of several convection rolls. Figure 7 shows that the temperature field also presents an oscillating dynamics but is however less affected than the concentration field. Experimentally a similar behavior called "rolling chemical wave," in which periodic convective motion of the tip of the front occurs in horizontal solution layers, has been observed with the autocatalytic chlorite-thiosulfate[12] and CT (Ref. 35) reactions in which solutal and thermal effects are competing.

1. Influence of the Rayleigh numbers

Let us first discuss the conditions on the Rayleigh numbers for this oscillatory dynamics to be observed, fixing the Lewis number to $Le=5$ and the solutal Rayleigh number to $R_C=-10$. As long as the thermal Rayleigh number is smaller than the solutal one ($|R_T|<|R_C|$), the density of the products $\rho_p=-R_C-R_T>0$ [cf. Eq. (12)]. The products are then globally heavier than the reactants with density $\rho_r=0$ and sink below them, giving rise to a steady propagating deformed front with constant shape[35] as seen in Fig. 9 for $R_T=5$. The thermal front is logically more spread out than the concentration front. There are three successive regions in the system, the first one behind the front corresponds to hot products, then the region of the front is constituted by cooled products below heated reactants due to the faster diffusion of heat, and lastly, the colder reactants at room temperature ahead of the front. Figure 10 shows the corresponding density and fluid velocity fields. We see that the maximum density corresponds to the solute heavier and cooled products at the bottom layer in the front deformation zone while the lightest solution is the solute lighter and heated reactants on top of them.

If $|R_T|=|R_C|$, the solute heavier but hotter products have the same density $\rho_p=0$ as the solute lighter reactants at room temperature ($\rho_r=0$). However, for $Le>1$, heat diffuses out of the products faster than mass near the front. The products which become locally rapidly heavier than the reactants therefore sink below them[35] giving rise to the same asymptotic situation as in Figs. 9 and 10. For $Le=5$ and $R_C=-10$, $R_T>13$ is needed to overcome this phenomenon

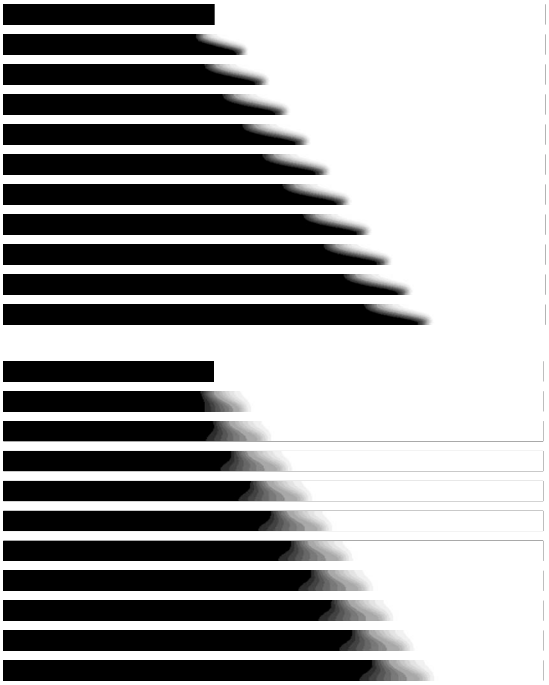

FIG. 9. Propagation of the concentration (top) and temperature (bottom) fronts in the presence of competing solutal and thermal buoyancy effects for $R_C=-10$, $R_T=5$, and $Le=5$ shown from top to bottom from $t=0$ up to $t=50$ with a time interval of $\Delta t=5$. The initial condition is at $x=100$ and the aspect ratio between $L_x=256$ and $L_z=10$ is preserved.

and to allow the products to stay globally lighter than the reactants long enough to rise on top of them and induce an oscillatory mechanism as depicted above.[35] The oscillation is superimposed on the deformation of the front across the layer (products on top of reactants), and the larger the thermal Rayleigh number, the more important the convection thereby resulting in a larger deformed front. The interface between reactants and products becomes nearly horizontal due to the large convective motions. Therefore, even if the products are initially much hotter and thus much lighter than the reactants ($R_T \gg 10$), oscillations can still occur because of the large horizontal extent of the interface across which heat can diffuse.

In both the steady and the oscillating regimes, the asymptotic properties (mixing lengths, constant propagation speed, and maximum fluid velocity) take smaller values when R_T gets closer to the threshold value between the two regimes. Eventually we note that similarly to the cooperative case, zones where the temperature exceeds the adiabatic value $T=1$ (hot spots) are still observed but are localized near the surface in the steady regime and everywhere across the layer in the oscillating regime. They are reminiscent of hot spots measured experimentally during fingering of the CT reaction in vertical systems.[36]

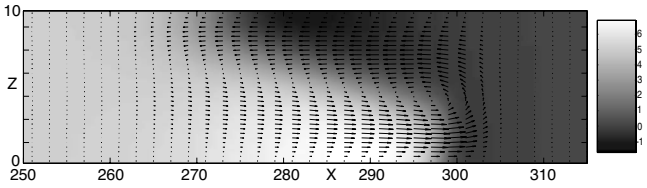

FIG. 10. Fluid velocity field in the front region superimposed on the density field shown at $t=100$ for the same parameters as in Fig. 9. As the density of the solution $\rho=-R_C c-R_T T$, the cold but solute lighter reactants ($c=0=T$) have a density $\rho_r=0.0$ while the hot but solute heavier products ($c=1=T$) have a density $\rho_p=5.0$. The density extrema exceed these values since, in the deformation zone, the heated reactants ($c\sim 0, T>0$) have an even smaller density, and the cooled products ($c\sim 1, T<1$) a still larger one. The density ranges indeed here from its minimum value, $\rho_{\min}=-1.24<\rho_r$, situated at the surface (heated reactants) shown in black to its maximum value, $\rho_{\max}=6.99>\rho_p$, situated at the bottom (cooled products) shown in white. As previously done, the z-direction has been magnified in order to see the details of the velocity field.

2. Influence of the Lewis number

As previously explained, the hot but solute heavier products rapidly lose their heat near the reaction front and sink below the reactants if the thermal Rayleigh number is not large enough compared to the solutal one ($R_T<13$ for $R_C=-10$ and $Le=5$). Since increasing the Lewis number corresponds to a larger diffusivity of heat, a larger difference between the thermal and solutal Rayleigh numbers is therefore needed to observe the oscillating dynamics. For example, an exothermic front characterized by $R_C=-10$ and $R_T=15$ presents an oscillating dynamics in the comoving frame for $Le=5$ (cf. Figs. 5–8) but the dynamics is steady for $Le\geq 10$. If we increase the difference between the Rayleigh numbers, the dynamics becomes oscillatory again. Indeed, fronts characterized by $Le=10$ and both $R_C=-10$, $R_T=20$ or $R_C=-5$, $R_T=15$ present oscillations in the comoving frame similar to the ones shown in Figs. 5–8.

Finally, the value of the asymptotic properties of the front, in both the steady and oscillating regimes, are increasing functions of the Lewis number oppositely to the cooperative situation. Indeed, for a same density jump between hot solute heavier products and cold solute lighter reactants, the intermediary reaction zone characterized by cold products beneath hot reactants (cf. Fig. 10) presents an even larger density difference when heat diffuses faster. The density gradients are of course more spread out but the major effect is the increase in the density difference arising from the fact that the products are more cooled down and the reactants more heated up when Le increases (see Fig. 11 showing density profiles on short times for $R_C=-10$ and $R_T=5$). For an oscillating situation as presented in Figs. 5–8, increasing the Lewis number results in a disappearance of the oscillations and the attainment of a steady regime.

IV. CONCLUSIONS

We have numerically characterized the influence of thermal effects on the nonlinear dynamics of exothermic autocatalytic chemical fronts propagating horizontally in the presence of buoyancy-driven convection induced by concentration and temperature gradients across the front. In the isothermal situation, the system attains an asymptotic dynamics characterized by a steady fluid vortex traveling at a constant speed with the deformed front.[23] We have here considered the influence of heat effects on such dynamics when the density difference across the front results from both a solutal contribution $\Delta\rho_s$ related to compositional changes in the course of reaction and a thermal contribution $\Delta\rho_T$ always

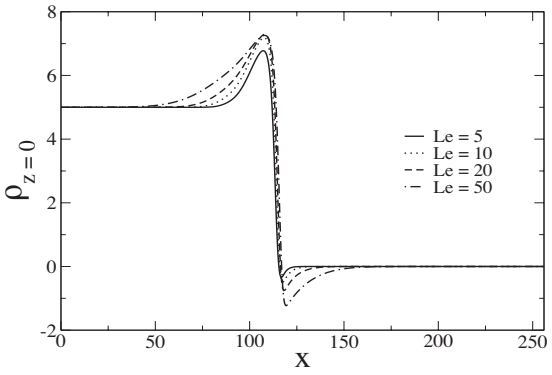

FIG. 11. One-dimensional density profiles along x plotted at the bottom of the layer ($z=0$) for $R_C=-10$, $R_T=5$ and various Lewis numbers ($t=5$). The density of the hot but solute heavier products (globally heavier) far behind the front is equal to $-R_C-R_T=5$ and the density of the cold but solute lighter reactants (globally lighter) is equal to 0 far ahead of the front. The density minimum corresponds to heated reactants (lighter than reactants at room temperature way ahead of the front) and the density maximum corresponds to cooled products (heavier than products way behind the front).

negative for exothermic autocatalytic reactions. Important changes are observed in the dynamics of exothermic systems with regard to the isothermal one. We have investigated two different situations: the first one where the solutal and thermal effects act cooperatively to decrease the density of the solution during the reaction, and the second one where they act antagonistically.

The difference between mass and heat diffusivities leads to new behaviors of the system even in the case of cooperative effects (hotter and solute lighter products) where, for some parameter range, we observe hot spots and a stabilization of a heavier solution on top of a lighter one at the rear of the front. The cooperative situation always leads to a steady asymptotic dynamics in a reference frame moving at a constant speed with the front. On the contrary, in the case of antagonistic effects (hotter but solute heavier products), a new oscillatory dynamics is observed when the overall density of the products is sufficiently smaller than that of the reactants i.e., $|R_T|$ is sufficiently larger than $|R_C|$ for a fixed Lewis number. Temporal oscillations of the concentration, temperature, and velocity fields can then occur in a frame of reference still moving at a constant speed with the front.

An interesting perspective would be to study the influence of the heat losses through the walls of the reactor on the dynamics of these exothermic fronts. Such heat losses have indeed been shown to affect the stability properties and nonlinear RDC dynamics of similar exothermic fronts propagating in vertical Hele-Shaw cells.[33,34,36]

ACKNOWLEDGMENTS

We thank N. Goyal and E. Meiburg for their help regarding the numerical integrations and T. Tóth, D. Horváth, and A. Tóth for fruitful discussions. L.R. is supported by a FNRS (Belgium) Ph.D. fellowship. A.D. acknowledges financial support from Prodex (Belgium), FNRS, and from the "Communauté française de Belgique" ("Actions de Recherches Concertées" program).

[1] J. A. Pojman and I. R. Epstein, J. Phys. Chem. **94**, 4966 (1990).
[2] J. A. Pojman, I. P. Nagy, and I. R. Epstein, J. Phys. Chem. **95**, 1306 (1991).
[3] B. F. Edwards, J. W. Wilder, and K. Showalter, Phys. Rev. A **43**, 749 (1991).
[4] J. D'Hernoncourt, A. Zebib, and A. De Wit, Chaos **17**, 013109 (2007).
[5] J. S. Turner, *Buoyancy Effects in Fluids* (Cambridge University Press, Cambridge, 1973).
[6] S. Kalliadasis, J. Yang, and A. De Wit, Phys. Fluids **16**, 1395 (2004).
[7] J. D'Hernoncourt, A. De Wit, and A. Zebib, J. Fluid Mech. **576**, 445 (2007).
[8] T. Bánsági Jr., D. Horváth, Á. Tóth, J. Yang, S. Kalliadasis, and A. De Wit, Phys. Rev. E **68**, 055301(R) (2003).
[9] T. Bánsági, Jr., D. Horváth, and Á. Tóth, Chem. Phys. Lett. **384**, 153 (2004).
[10] T. Tóth, D. Horváth, and Á. Tóth, Chem. Phys. Lett. **442**, 289 (2007).
[11] J. D'Hernoncourt, A. Zebib, and A. De Wit, Phys. Rev. Lett. **96**, 154501 (2006).
[12] I. Nagypál, G. Bazsa, and I. R. Epstein, J. Am. Chem. Soc. **108**, 3635 (1986).
[13] J. A. Pojman, I. R. Epstein, T. J. McManus, and K. Showalter, J. Phys. Chem. **95**, 1299 (1991).
[14] I. P. Nagy, A. Keresztessy, J. A. Pojman, G. Bazsa, and Z. Noszticzius, J. Phys. Chem. **98**, 6030 (1994).
[15] A. Keresztessy, I. P. Nagy, G. Bazsa, and J. A. Pojman, J. Phys. Chem. **99**, 5379 (1995).
[16] M. Belk, K. G. Kostarev, V. Volpert, and T. M. Yudina, J. Phys. Chem. B **107**, 10292 (2003).
[17] M. J. B. Hauser and R. H. Simoyi, Chem. Phys. Lett. **227**, 593 (1994).
[18] B. S. Martincigh and R. H. Simoyi, Phys. Rev. E **52**, 1606 (1995).
[19] C. R. Chinake and R. H. Simoyi, J. Chem. Soc., Faraday Trans. **93**, 1345 (1997).
[20] B. S. Martincigh and R. H. Simoyi, J. Phys. Chem. **106**, 482 (2002).
[21] T. Plesser, H. Wilke, and K. H. Winters, Chem. Phys. Lett. **200**, 158 (1992).
[22] D. A. Vasquez, J. M. Littley, J. W. Wilder, and B. F. Edwards, Phys. Rev. E **50**, 280 (1994).
[23] L. Rongy, N. Goyal, E. Meiburg, and A. De Wit, J. Chem. Phys. **127**, 114710 (2007).
[24] L. M. Pismen, Phys. Rev. Lett. **78**, 382 (1997).
[25] L. Rongy and A. De Wit, J. Chem. Phys. **124**, 164705 (2006).
[26] L. Rongy and A. De Wit, J. Eng. Math. **59**, 221 (2007).
[27] L. Rongy, A. De Wit, and G. M. Homsy, Phys. Fluids **20**, 072103 (2008).
[28] A. Pereira, P. M. J. Trevelyan, U. Thiele, and S. Kalliadasis, Phys. Fluids **19**, 112102 (2007).
[29] A. Hanna, A. Saul, and K. Showalter, J. Am. Chem. Soc. **104**, 3838 (1982).
[30] *Oscillations and Traveling Waves in Chemical Systems*, edited by R. J. Field and M. Burger (Wiley, New York, 1985).
[31] K. Showalter, in *Kinetics of Nonhomogenous Processes*, edited by G. R. Freeman (Wiley, New York, 1987), p. 769.
[32] A. De Wit, Phys. Rev. Lett. **87**, 054502 (2001).
[33] J. D'Hernoncourt, S. Kalliadasis, and A. De Wit, J. Chem. Phys. **123**, 234503 (2005).
[34] J. D'Hernoncourt and A. De Wit, "Influence of heat losses on nonlinear fingering dynamics of exothermic autocatalytic fronts," Physica D (in press).
[35] L. Rongy, G. Schuszter, Z. Sinkó, T. Tóth, D. Horváth, A. Tóth, and A. De Wit, Chaos **19**, 023110 (2009).
[36] P. Grosfils, F. Dubois, C. Yourassowsky, and A. De Wit, Phys. Rev. E **79**, 017301 (2009).